

FULL MOMENT TENSOR ANALYSIS USING FIRST MOTION DATA AT THE GEYSERS GEOTHERMAL FIELD

O. S. Boyd¹, D. S. Dreger¹, V. H. Lai¹ and R. Gritto²

¹Berkeley Seismological Laboratory
University of California, Berkeley
Berkeley, California, 94720, USA
e-mail: sierra@seismo.berkeley.edu

²Array Information Technology
2020 Cedar Street
Berkeley, California 94709, USA

ABSTRACT

Seismicity associated with geothermal energy production at The Geysers Geothermal Field in northern California has been increasing during the last forty years. We investigate source models of over fifty earthquakes with magnitudes ranging from Mw 3.5 up to Mw 4.5. We invert three-component, complete waveform data from broadband stations of the Berkeley Digital Seismic Network (BDSN), the Northern California Seismic Network (NCSN) and the USA Array deployment (2005-2007) for the complete, six-element moment tensor. Some solutions are double-couple while others have substantial non-double-couple components. To assess the stability and significance of non-double-couple components, we use a suite of diagnostic tools including the F-test, Jackknife test, bootstrap, and network sensitivity solution (NSS). The full moment tensor solutions of the studied events tend to plot in the upper half of the Hudson source type diagram where the fundamental source types include +CLVD, +LVD, tensile-crack, DC and explosion. Using the F-test to compare the goodness-of-fit values between the full and deviatoric moment tensor solutions, most of the full moment tensor solutions do not show a statistically significant improvement in fit over the deviatoric solutions. Because a small isotropic component may not significantly improve the fit, we include first motion polarity data to better constrain the full moment tensor solutions.

METHODOLOGY

The objective is to determine the best fitting source model and then evaluate the significance and resolution of possible non-double-couple source types that might arise from fluid-related processes in

the geothermal system.

Over fifty events from 1992 through 2012 were selected from the UC Berkeley Moment Tensor Catalog, as listed in Table 1 of the Appendix. An initial review of moment tensor solutions for the selected events is accomplished using the UC Berkeley Moment Tensor Interface, a flexible web-based system that drives the full moment tensor inversion code. Broadband seismic data are downloaded from stations of multiple seismic networks to expand azimuthal coverage. Preprocessing of the seismic data includes removing the instrument response, integrating to ground displacement and filtering the data. We first obtain a deviatoric solution followed by a full moment tensor solution for comparison. Selected solutions are shown in Figure 1.

The moment tensor interface allows flexibility in choosing several velocity models, including the GIL7 (e.g. Pasyanos et al., 1996) and the social 1D velocity model (Dreger and Helmberger, 1993), and filtering options. Synthetic waveforms are generated using FKRPORG at a range of shallower depths including 1.5, 3.5, 5.0, 8.0, up to a depth of 39.0 km. We find that depth sensitivity using data filtered between 0.02 to 0.05 Hz is limited, so we therefore restrain our analysis to event depths determined from the NCSS catalog. In the future with better calibrated velocity models, and/or using the local Calpine seismic data we may be able to improve on moment tensor based source depth determination. However for now we assume that the depths reported in the catalog are well determined and focus on the recovery of the seismic moment tensor source parameters. The observed and synthetic waveforms for each station

are shifted until a maximum goodness-of-fit, also known as the variance reduction (VR), is obtained.

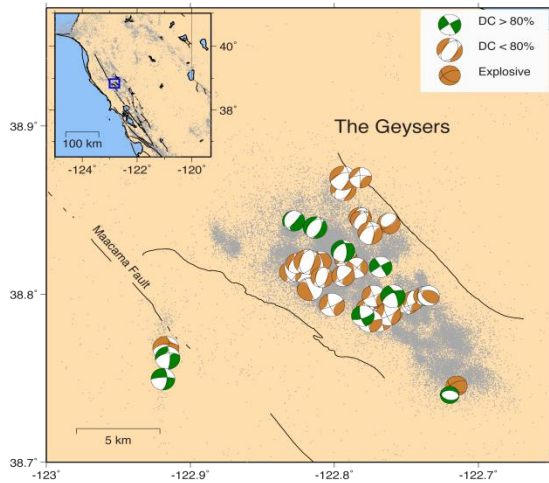


Figure 1. Map showing seismicity and selected moment tensor solutions at The Geysers Geothermal Field.

We have worked to develop a systematic procedure for the evaluation of aleatoric and epistemic solution uncertainty (e.g. Ford et al., 2009; Ford et al., 2010). Several methods were used to assess solution stability and the significance of the non-double-couple terms:

- 1) The F-Test is used to evaluate significance of improved fit with higher degrees of freedom.
- 2) A Jackknife test using various groups of stations is used to identify problematic source-receiver paths requiring additional velocity model calibration
- 3) A Bootstrap procedure is used to estimate aleatoric uncertainty.
- 4) The Network Sensitivity Solution (NSS; Ford et al., 2010) is used to quantify uncertainty of the source type parameters.
- 5) First motion polarity data is used to constrain the full moment tensor solution.

Preliminary results indicate that the October 12, 1996 earthquake has a large isotropic component that appears to be stable and suggestive of fluid or gas involvement during the rupture processes. In addition, the March 1, 2011 earthquake appears to have a moderate isotropic component when constrained using the first motion polarity data.

October 12 1996 Earthquake

The full moment tensor solutions were computed for each of the studied events and are listed in Table 2 of the Appendix. However, only one full moment tensor solution yielded a statistically significant result and is

listed in Table 2 for event October 12, 1996 with a 57 percent isotropic component.

The F-test confidence level of significance is 99.9 percent. The full moment tensor solution for this earthquake is shown in Figure 2. The observed waveforms are plotted with solid black lines and the synthetic waveforms are shown with dashed lines.

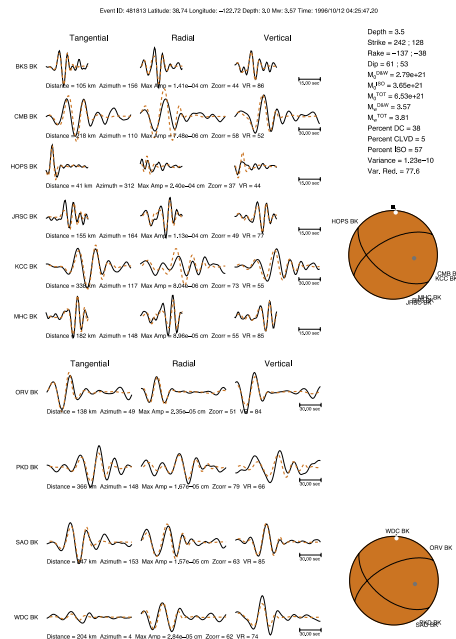


Figure 2. The full moment tensor solution for the October 12, 1996 earthquake.

Ten stations ranging in distance from 40 to 330 km were used in this initial moment tensor computation. The plotted waveforms show differences in filtering bands and correlation intervals as indicated by the different time scales shown under the plot of the vertical components. In general, higher frequencies were allowed for stations within 100 km.

This event is unusual with respect to other studied events in that the deviatoric solution appears to have a east-west striking normal faulting mechanism, similar to the nearby beachball in the southeast corner of Figure 1. Likewise, the full moment tensor solution is unusual in that it appears to require a component of volume increase. First motions indicate that the volume increase is secondary.

March 1, 2011 Earthquake

For this earthquake we carefully reviewed the first arrival polarities and used them jointly with the waveform data to further constrain the moment tensor solution. The first motion polarity data include the

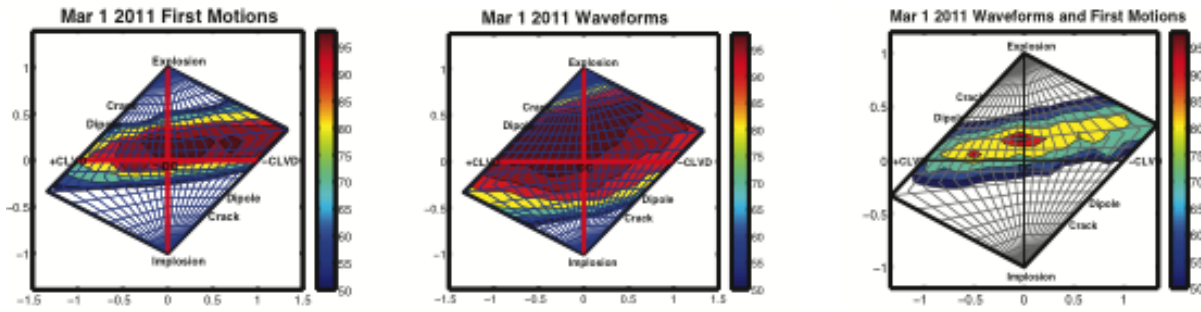


Figure 3. Source type plots of network sensitivity solutions using first motion polarity data, waveform data and combined datasets.

azimuth, take-off angle, polarity (up or down) and a weighting factor for selected stations culled from a list generated by the USGS. In many instances the first motions resulted from the arrival of head waves warranting careful evaluation using various tools including Seismic Analysis Code (SAC) and Jiggle software from the USGS.

Figure 3 shows three source-type plots of network sensitivity solutions (NSS) using (a) first motion polarity data, (b) waveform data, and (c) combined first motion polarity and waveform data. These source-type plots show the goodness-of-fit values for various moment tensor solutions using the datasets specified above. Higher goodness-of-fit values are indicated with warmer colors. Moment tensor solutions having a high double-couple (DC) component plot in the center; solutions having some proportion of a compensated linear vector dipole (CLVD) component plot along the horizontal axis, and those having a volumetric isotropic (ISO) component plot either above or below the horizontal axis such that explosive/implosive solutions plot towards the upper/lower regions, respectively. We used a parallel version of the NSS code to test 200 million possible moment tensor solutions using the waveform data. Most of the waveform solutions were rejected due to negative fit values. The region indicating the best NSS solutions using the combined datasets is significantly reduced and localized.

Figure 4 compares observed waveforms (black) to those modeled (red) using the best-fitting moment tensor solution with the combined first motion polarity and waveform data. Values of strike, rake, dip, moment, percent DC, percent CLVD, percent ISO components and goodness-of-fit (variance reduction) are shown along with the focal mechanism using the combined datasets.

Figure 5 shows the first motion polarity data (green + down, black + up) superimposed on various focal mechanisms. The size of the first motion polarity

symbol indicates the weight given to the first motion pick with a larger size denoting higher confidence.

The first focal mechanism is the best-fitting focal mechanism using the combined datasets. The middle and last focal mechanisms are the full/deviatoric moment tensor solutions from the BSL database. Good agreement between the first motion polarity data and focal mechanism occurs when the green + (down) symbols coincide with the white dilational regions, and the black + (up) symbols coincide with the red shaded compressional regions. Goodness-of-fit values are listed in the figure captions.

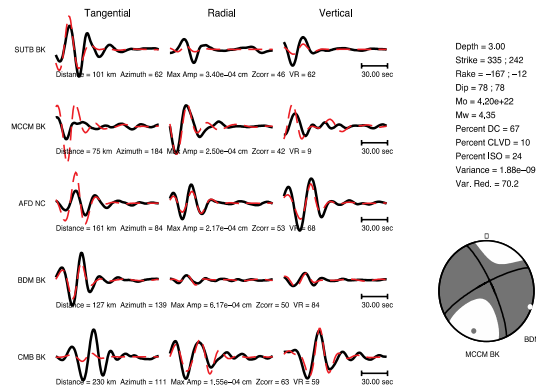


Figure 4. Comparison of observed waveforms (black) with those modeled (red) using the best-fit moment tensor solution with the combined datasets. The percent components of DC, CLVD and ISO are 67%, 10% and 24%, respectively, for the modeled solution.

It is noteworthy that the first motion data are not fit by the deviatoric waveform solution. On the other hand there is substantially improved fit to the first motions using the full moment tensor solution. As shown the best fit to the first motions is for the combined NSS result (Figure 5a). There is an acceptable level of fit to the waveform data for this mechanism as shown in Figure 4.

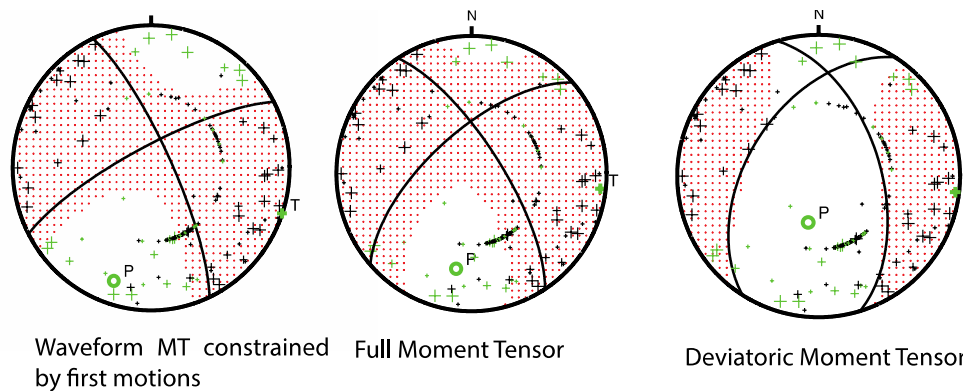


Figure 5. Shown here are overlays of the first motion polarity picks (green + down; black + up) on the following focal mechanisms: joint waveform and first motion polarity, full, and deviatoric moment tensor solutions. White regions are dilatational and red regions are compressional. The goodness-of-fit values for agreement between the first motion polarity data and the focal mechanisms are 70%, 25% and -6%, respectively, suggesting the moment tensor solution using the combined datasets fits well with the first motion polarity data.

CONCLUSIONS AND DISCUSSION

We have determined source parameters and uncertainties of over fifty $M > 3.5$ earthquakes at The Geysers Geothermal Field using a regional moment tensor method. We invert three-component, complete waveform data from broadband stations of the BDSN, NCSN and USA Array deployment (2005-2007) for deviatoric and full, six-element moment tensor solutions. The six-element full moment tensor solution includes the isotropic component and is representative for source processes with a volumetric response and is considered for all of the studied events. The fits are the same or higher when more degrees of freedom are used compared to the deviatoric solutions. However, the full moment tensor solution for the October 12, 1996 event is statistically significant with a 99.9% confidence level of significance as determined with the F-test. This initial analysis has defined the framework with which we will determine and review moment tensor solutions for $M > 3$ seismicity occurring in the region.

First motions for the October 12, 1996 event reveal that the volumetric source is secondary to the normal-type shear dislocation. This could result from thermally induced tensile stress driving additional failure after the rocks are weakened through shearing.

The F-test evaluates whether the improved fit afforded by the additional degree of freedom is statistically significant considering the amount of uncorrelated data used in the inversion. If a volumetric term is a small fraction of the total

seismic moment then the change in fit will be small, and the F-test will not provide a good measure of the significance of the result. It is in these cases that first motion data may provide the needed additional constraint to determine whether the small volumetric component is real. The March 1, 2011 event demonstrates this. Based on the F-test measure we would interpret the waveform moment tensor result to be the deviatoric solution rather than the full moment tensor solution. The deviatoric solution fails to fit the first motions, while there is a marked improvement when the full moment tensor solution is considered. The preferred mechanism in this case is the solution obtained by considering the intersection of the first motion and waveform NSS model spaces.

ACKNOWLEDGEMENTS

This work is supported by the Department of Energy Geothermal Technologies Program under Award Number DD-EE0002756-002. We also thank A.Chiang, A. Guilhem and S.H. Yoo for their support.

REFERENCES

- Dreger, D. S., and D. V. Helmberger (1993), Determination of Source Parameters at Regional Distances with Single Station or Sparse Network Data, *Journ. Geophys. Res.*, **98**, 8107-8125.
- Ford, S. R., D. S. Dreger and W. R. Walter (2009). Identifying isotropic events using a regional moment tensor inversion, *J. Geophys. Res.*, **114**, B01306, doi:10.1029/2008JB005743.

Ford, S. R., D. S. Dreger and W. R. Walter (2010). Network sensitivity solutions for regional moment tensor inversions, *Bull. Seism. Soc. Am.*, **100**, p. 1962-1970.

Pasyanos, M. E., D. S. Dreger, and B. Romanowicz (1996). Toward real-time estimation of regional moment tensors, *Bull. Seism. Soc. Am.* **86**, 1255-1269.

Table 2. Preliminary full moment tensor solutions of studied events.

No.	Ev ID	Mxx E+20	Mxy E+20	Mxz E+20	Myy E+20	Myz E+20	Mzz E+20	%DC	%CLVD	%ISO	VR FMT	F-sig
1	316220	334.520	-462.69	78.379	800.25	-81.971	1072.5	14	30	56	68.7	72.46
2	332712	41.941	-42.014	-20.017	128.26	30.831	148.98	38	5	57	75.2	81.52
3	332716	27.41	-19.596	6.654	61.153	-0.861	95.54	24	15	61	68.2	85.72
4	337179	-22.575	-60.832	11.315	82.58	8.271	42.057	54	16	29	73.8	46.87
5	340271	-6.582	-113.68	-28.482	119.83	26.893	118.17	43	21	36	70.3	47.17
6	375872	-9.171	11.379	-79.167	109.7	26.696	-68.005	46	46	8	80.1	72.12
7	30036258	-73.508	-45.373	10.406	112.73	4.81	45.529	53	25	21	73.8	47.39
8	30056092	30.641	-29.757	14.161	118.68	15.64	83.361	31	11	58	75.2	61.48
9	30066289	216.86	-90.934	53.979	365.28	96.869	482.75	27	8	65	68.9	76.22
**10	481813	63.023	3.415	4.213	26.147	-14.721	20.183	38	5	57	77.6	99.99
11	30121914	-23.365	-32.222	-13.797	92.337	8.57	-53.07	31	63	6	69.3	47.57
12	486680	-98.418	-198.44	170.34	446.34	81.848	387.36	11	50	40	81.7	85.01
13	30180424	-0.637	-26.24	-24.798	48.864	7.499	-8.062	59	19	22	68	54.09
14	30217691	13.43	-132.08	15.397	333.88	-15.562	233.57	35	17	48	64.8	73.25
15	21006582	3.751	-10.265	-83.538	80.353	31.699	-19.165	41	42	18	50.8	51.21
16	21038803	-14.439	-5.841	-3.578	46.901	11.887	-17.032	13	75	13	64.5	47.16
17	21076021	-17.129	-23.014	-49.39	21.703	54.08	-84.99	74	4	22	57.8	53.03
18	21076620	42.456	-304	78.688	201.53	182.08	45.049	72	8	20	77.6	69.34
19	21076750	153.75	-703.06	358.47	381.78	434.33	28.788	50	32	17	73.9	48.45
20	21078341	-10.405	-206.79	103.99	-23.992	40.323	-189.96	58	19	23	82.1	46.87
21	21090381	-9.058	14.51	-60.797	55.424	36.925	-4.016	31	53	15	59.7	50.74
22	21137862	-145.71	-185.26	94.414	474.86	210.61	286.4	60	8	32	84.8	63.53
23	21221952	15.121	-83.406	-30.514	130.24	-28.552	135.13	15	39	46	80.2	70.82
24	21225043	-37.757	-21.921	8.825	26.174	22.155	-18.419	58	24	18	59.6	53.98
25	30225804	-44.616	99.225	-195.71	-82.731	-443.84	-212.43	77	4	18	41.6	54.66
26	30226108	22.168	-113.43	7.254	241.45	8.936	213.02	21	29	50	74.6	84.52
27	30226367	263.66	-91.687	8.126	368.6	27.374	448.89	8	18	74	70.5	74.76
28	21344222	410.36	-231.56	72.907	832.15	146.1	922.62	16	18	65	69.7	97.82
29	21415559	2.218	-76.283	-1.425	145.99	-23.705	95.517	47	10	43	82.7	66.36
30	21455621	-78.979	-255.15	-24.075	501.17	-8.665	276.25	49	14	38	85.5	88.49
31	21495369	-30.852	4.023	-19.448	62.147	10.191	-2.673	75	10	15	54.4	67.49
32	21516950	-64.895	-555.73	93.29	1513.6	-161.76	376.98	33	28	38	76.8	61.12
33	21543835	446.87	-826.82	164.37	775.17	27.06	399.97	46	15	39	82.2	65.26
34	21544051	24.483	-66.563	-14.81	43.48	22.41	25.74	45	24	30	76.6	46.68
35	51181154	-38.715	-353.58	36.721	635.46	19.404	577.27	18	49	34	80.6	47.81
36	51184307	28.896	-34.583	-6.783	149.09	8.637	180	12	29	59	68.6	61.90
37	40206647	-11.034	-32.963	-76.038	144.84	-8.414	-11.453	51	23	25	65.7	50.56
38	51197011	23.923	-64.288	-2.74	145.1	31.093	93.28	48	3	48	56.6	45.80
39	51199197	-7.921	-14.033	-2.919	22.753	2.694	2.857	55	23	22	62.1	59.86
40	40218402	-21.805	-161.97	25.62	222.85	-26.233	79.968	57	12	31	80.1	57.28
41	51214595	-19.07	-296.34	-87.279	148.2	33.203	107.11	74	7	20	78.5	67.45
42	71346081	3.948	-8.794	-6.905	30.924	-2.91	-20.924	80	6	14	61	51.67
43	71425345	0.36	-103.74	3.68	100.08	14.681	52.672	67	2	31	73.2	52.90
44	71425825	-34.321	-33.114	-21.494	66.571	-18.146	-63.548	56	33	12	68.5	51.07
45	71530230	-48.777	-80.386	195.72	717.01	172.16	-1.145	54	15	31	75.7	58.86
46	71576830	-51.511	11.992	-11.028	38.237	7.7	-39.818	34	39	26	55.7	48.19
47	71592270	16.905	1.895	1.291	6.866	-1.474	5.689	18	21	60	49	52.57
48	71720790	-6.054	-4.012	-6.922	3.162	2.153	-17.06	52	14	34	47.8	55.79
49	71729135	-84.308	-146.71	-7.062	231.86	6.046	-7.044	46	37	18	72.6	72.58
50	71776130	-176.53	-62.976	-25.869	386.79	-58.942	147.59	62	9	29	75.8	
51	71813266	-19.822	-11.132	-37.006	75.839	14.566	-48.198	94	4	4	76.3	